Assessment of beryllium and molybdenum nuclear data files with the RPI neutron scattering system in the energy region from 0.5 to 20 MeV

Adam Daskalakis[1,2,a], Ezekiel Blain[1], Gregory Leinweber[2], Michael Rapp[2], Devin Barry[2], Robert Block[2], and Yaron Danon[1]

[1] Rensselaer Polytechnic Institute, Gaerttner LINAC Center, 110 8thSt., Troy, NY 12180, USA
[2] Bechtel Marine Propulsion Corp., Knolls Atomic Power Laboratory, PO Box 1072, Schenectady, NY 12301-1072, USA

Abstract. A series of neutron scattering benchmark measurements were performed on beryllium and molybdenum with the Rensselaer Polytechnic Institute's Neutron Scattering System. The pulsed neutron source was produced by the Rensselaer Polytechnic Institute's Linear Accelerator and a well collimated neutron beam was incident onto the samples located at a distance of 30.07 m. Neutrons that scattered from the sample were measured using the time-of-flight by eight EJ-301 liquid scintillator detectors positioned 0.5 m from the sample of interest. A total of eight experiments were performed with two sample thicknesses each, measured by detectors placed at two sets of angles. All data were processed using pulse shape analysis that separated the neutron and gamma ray events and included a gamma misclassification correction to account for erroneously identified gamma rays. A detailed model of the neutron scattering system simulated each experiment with several current evaluated nuclear data libraries and their predecessors. Results for each evaluation were compared to the experimental data using a figure-of-merit. The neutron scattering system has been used as a means to quantify a library's performance.

1. Introduction

Over the past decade several neutron scattering experiments were performed at the Rensselaer Polytechnic Institute (RPI) Gaerttner Linear Accelerator (LINAC) Facility [1–5]. The RPI neutron scattering system was designed to benchmark the cumulative effects from neutron scattering from a sample. A term commonly used to describe this measurement is "quasi-differential" neutron scattering due to several factors: thick samples increased the probability of multiple scattering events; detectors were positioned close to the scattering samples to improve signal strength; and the neutron source produced neutrons with a wide range of energies [1]. These features reduced experimental uncertainty by improving the neutron count rate over a range of neutron energies in the region of interest (ROI), 0.5 and 20 MeV. Scattering measurements were performed with beryllium-9 [2], elemental molybdenum [2], elemental zirconium [1], uranium-238 [3], elemental iron [4], and elemental lead [5]. Each of these measurements compared the experimental data to MCNP simulations that modeled evaluated nuclear data libraries such as ENDF/B-VII.1 [6], JEFF-3.2 [7], or JENDL-4.0 [8].

^{9}Be and ^{Nat}Mo scattering experiments [2] were reanalyzed with updated methods and techniques to better correlate experimental data with calculations [3]. For both experiments detectors were positioned at eight unique angles. Two sample thicknesses were used; the thicker one had a higher probability for multiple collisions. The ^{9}Be sample thicknesses were 4 cm and 8 cm; ^{Nat}Mo samples were 5 cm and 8 cm thick.

2. Experimental setup

The RPI LINAC generates electrons with energies up to 60 MeV in order to collide them with a neutron-producing tantalum target. Bremsstrahlung radiation produced within the target by high energy electrons interacts with tantalum plates and creates neutrons through the (γ,n) reaction. Neutrons are produced with a continuous energy distribution similar to an evaporation spectrum with a temperature of 0.46 MeV. For all scattering experiments the LINAC was operated at 400 pulses per second with an average current on target of 8 μA with an electron burst width of approximately 8 ns. Moderated fission chambers positioned ≈ 9 m from the neutron-producing target monitored fluctuations in neutron beam intensity. Evacuated flight tubes were positioned between the neutron-producing target and scattering samples. Collimators placed within the flight tubes reduced the neutron beam diameter to ≈ 7.6 cm at the location of the scattering sample. Additionally, detector locations were chosen to maximize the distance between detectors and from vacuum tubes to limit scattering contribution from all sources except the scattering sample.

The detectors used by the RPI Neutron Scattering System were EJ-301 proton recoil fast neutron liquid scintillators that were coupled to Photonis XP4572/B photomultiplier tubes (PMT). Detector details and modeling parameters were previously described in [2–4].

[a] e-mail: adam.daskalakis@unnpp.gov

Table 1. Scattering sample properties.

Sample	Diameter [cm]	Mass [g]
Graphite – 7 cm	7.498 ± 0.003	521.87 ± 0.01
^{9}Be – 4 cm	7.503 ± 0.003	326.61 ± 0.01
^{9}Be – 8 cm	7.501 ± 0.003	653.06 ± 0.01
^{Nat}Mo – 5 cm	7.616 ± 0.001	2411.9 ± 0.1
^{Nat}Mo – 8 cm	7.615 ± 0.001	3713.4 ± 0.1

Detector positions (angles relative to the incident neutron beam) were selected based on several criteria, including discrepancies between different nuclear data libraries, as described in [1]. All signals from a detector were passed to an Agilent-Acqiris AP240 digitizer. If a signal exceeded a predefined threshold, the signal was converted to a digitized event. Each digitized event consisted of 120 8-bit data points with a time-stamp used to calculate its time-of-flight (TOF). The TOF scattering experiment was previously discussed in [3].

Neutron events were distinguished from gamma-ray events using a shape analysis (PSA) technique that categorized a digitized pulse as a neutron or gamma ray based on its fit relative to reference neutron and gamma ray shapes [4]. A small fraction of gamma rays were erroneously identified as neutrons due to limitation of the PSA method and were corrected for by another method described in Ref. [4]. In past experiments, where fission was present, this was determined to be approximately 3% between 5 and 20 MeV [3].

3. Data collection and analysis

Several sets of data were collected for each experiment. Each consisted of the sample of interest (either ^{9}Be or ^{Nat}Mo), a graphite reference sample, and an open beam (background) measurement. The samples are described in Table 1. Throughout an experiment the sample of interest and the graphite reference sample were cycled in and out of the neutron beam. Open beam was measured when no sample was positioned in the neutron beam. Approximately 36 cycles were performed for each experiment, with a single measurement lasting under 20 minutes [2].

For each experiment neutron counts, $C_{i,j}$, for the sample of interest or graphite reference sample were determined from Eq. (1),

$$\mathrm{C_{ij}} = (\mathrm{D^{S}_{ij}} - \mathrm{G^{S}_{ij}}) - (\mathrm{D^{O}_{ij}} - \mathrm{G^{O}_{ij}}) \cdot \frac{\mathrm{M^{S}}}{\mathrm{M^{O}}}. \qquad (1)$$

The counts, $C_{i,j}$, measured from the scattering sample, $D^{S}_{i,j}$, and open beam, $D^{O}_{i,j}$, were corrected by their erroneous gamma-ray contribution, $G^{S}_{i,j}$ and $G^{O}_{i,j}$, respectively. Neutron monitors were used to correct for fluctuations in beam intensity by adjusting the open beam counts using the ratio of monitor counts with the sample, M^2, to the monitor counts with the open beam, M^O. This process was performed for each detector i and at each energy interval j. Statistical uncertainty was determined from the standard error propagation formula for uncorrelated variables [9] and previously derived in [3].

MCNP calculations were directly compared with data from the samples of interest and the graphite reference sample. Each calculation modeled structural material, a neutron source, and the detector responses. The neutron source and detector responses were determined from a series of in-beam measurements and MCNP simulations [3]. The neutron source term and the individual detector efficiencies were incorporated into all MCNP simulations performed for this work.

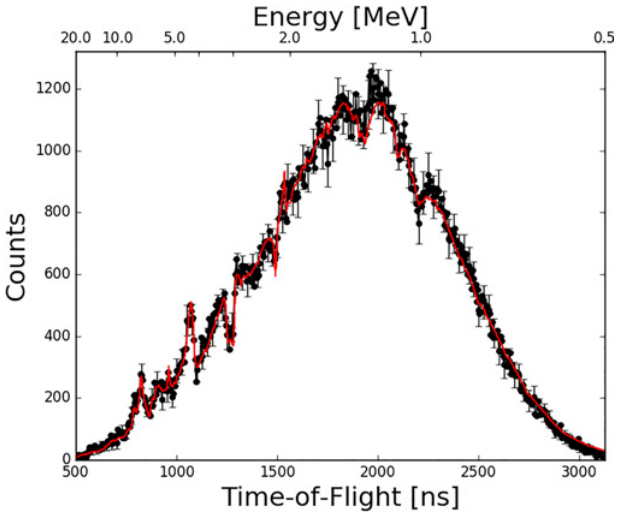

Figure 1. Graphite reference sample data for a detector positioned at 52°. Agreement between the graphite reference sample and the MCNP calculation was used to obtain the systematic uncertainty.

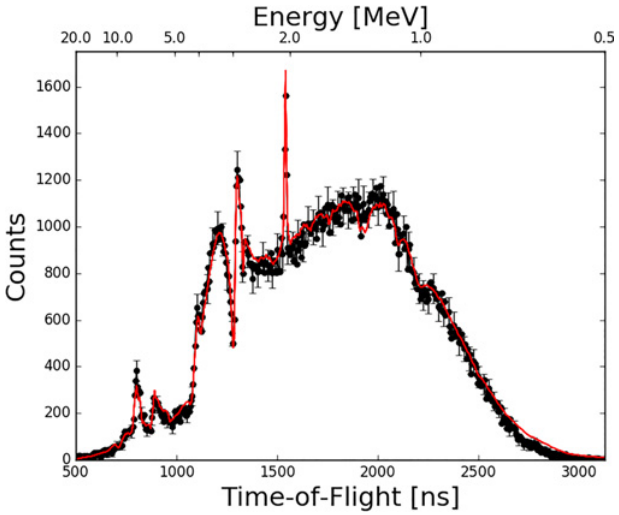

Figure 2. Graphite reference sample for a detector positioned at 140°. Agreement between the graphite reference sample and the MCNP calculation was used to obtain the systematic uncertainty.

Data from the graphite reference sample and its associated MCNP simulation were used to normalize all MCNP calculations to experimental data. Agreement between experimental graphite data and calculations are shown in Figs. 1 and 2. This process was previously described in Ref. [3].

A figure-of-merit (FOM) with the same functional form as a reduced chi-square goodness of fit was used to compare the experimental data to MCNP simulations. The FOM was previously described in [3]. The equation for the FOM is given in Eq. (2),

$$\mathrm{FOM_{i,j}} = \frac{1}{\mathrm{n}} \sum_{0.5\,\mathrm{MeV}}^{20\,\mathrm{MeV}} \frac{(\mathrm{C_{i,j}} - \mathrm{MC_{i,j}})^2}{\varepsilon_{\mathrm{i,j}}{}^2} \qquad (2)$$

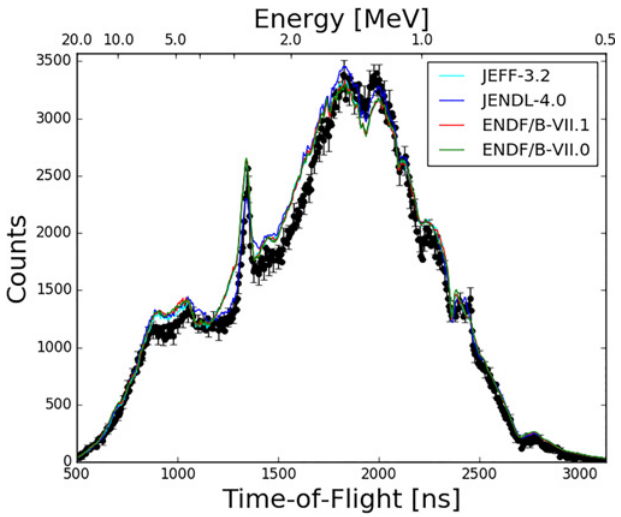

Figure 3. ^{9}Be for a detector positioned at 51°. Significant differences were observed between 2 and 4 MeV. The 4 cm thick beryllium sample was used for this measurement.

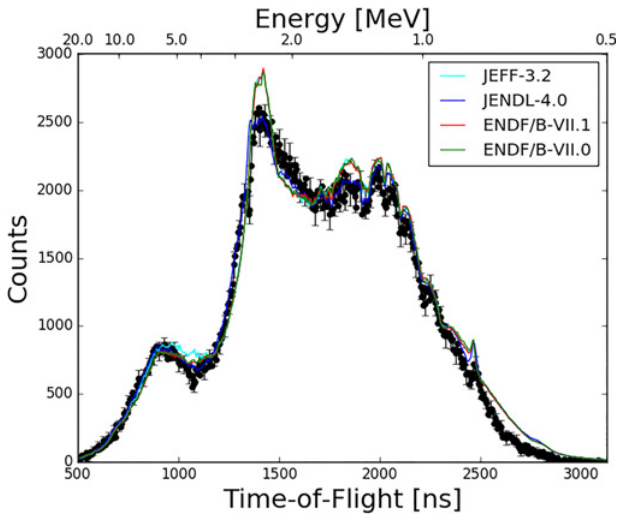

Figure 4. ^{9}Be for a detector positioned at 140°. Significant differences were observed around 1.5 MeV and between 2 and 3 MeV. The 4 cm thick beryllium sample was used for this measurement.

Table 2. Average figures of merit, FOM, for the beryllium measurements. Bolded values represent the best fits.

Library	^{9}Be – 4 cm	^{9}Be – 8 cm
ENDF/B-VII.1	2.14	2.38
ENDF/B-VII.0	2.19	2.46
JEFF-3.2	2.17	2.40
JENDL-4.0	**1.89**	**2.15**
Graphite	1.40	1.40

Table 3. Average figures of merit, FOM, for the molybdenum measurements. Bolded values represent the best fits.

Library	^{Nat}Mo – 5 cm	^{Nat}Mo – 8 cm
ENDF/B-VII.1	**2.08**	**2.00**
JEFF-3.2	2.12	2.05
JENDL-4.0	2.28	2.53
Graphite	1.61	1.47

where the numerator is the squared difference between experimental data, $C_{i,j}$, and the MCNP simulation, $MC_{i,j}$, for each detector, i, and each evaluation, j. The denominator contains the uncertainty, $\varepsilon_{I,J}$, which is the sum of the statistical uncertainty (standard error propagation) and the systematic uncertainty [3]. For a given detector and experiment the calculated FOMs from various libraries were directly compared to each other. The library with the lowest FOM was deemed best fitting. If the calculated FOM for the sample of interest was greater than the FOM for the graphite reference sample performance could improve. Otherwise, it was deemed to perform better than the graphite reference sample indicating that the differentiation between libraries for that particular detector could not be made.

4. Beryllium results

For both sets of experiments, the average FOM for the graphite reference sample was 1.40. FOMs for ENDF/B-VII.1, ENDF/B-VII.0, JEFF-3.2, and JENDL-4.0 compared to the average values from 14 measurements are shown in Table 2. The graphite FOM was lower than ^{9}Be FOM, which indicates that all libraries could be improved to better agree with the experimental data. On average the best fitting library is JENDL-4.0.

^{9}Be data and MCNP calculations are plotted in Fig. 3 and Fig. 4 for a detector positioned at 51° and 140°, respectively. These are the same detectors shown in Figs. 1 and 2. The results for both ^{9}Be thicknesses show that the JENDL-4.0 library had the best agreement with experimental data collected by detectors positioned at 26°, 52°, 73°, 90°, 140°, and 154°. The exceptions were for detectors positioned at 108° and 118°, where ENDF/B-VII.1 performed better. Additionally, for all libraries, the average FOM was larger for the thicker sample, implying that additional scattering events compounded differences between experimental data and MCNP simulations.

In general, the ENDF/B libraries did not agree with the experimental data as well as the JENDL-4.0 library. The ENDF/B-VII.1 did perform better than ENDF/B-VII.0, which had the poorest agreement. The only region that the ENDF/B-VII.1 library performed well was for detectors positioned at ≈ 110°.

Lastly, the JEFF-3.2 library performed nearly on par with the ENDF/B-VII.1 library. Its average FOM was larger than the ENDF/B-VII.1; however, it performed better than the ENDF/B-VII.0 library. There were no measurements where the FOM had the JEFF-3.2 library with the best agreement.

5. Molybdenum results

The FOMs for the graphite reference sample were 1.61 and 1.47 during the 5 cm and 8 cm Mo measurements, respectively, as shown in Table 3. This is larger than 1.40 reported with the ^{9}Be experiment. As a result, the graphite FOM was larger than the ^{Nat}Mo FOM for some detectors and libraries. Therefore, these libraries were in agreement with the experimental datasets. The ENDF/B-VII.1 library had the best agreement with the experimental molybdenum data.

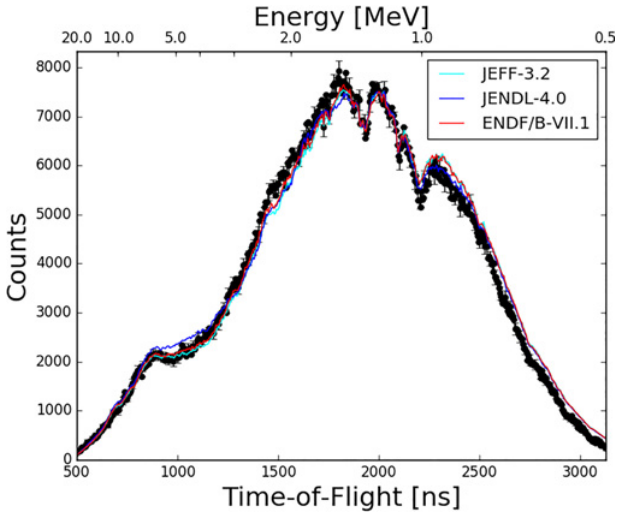

Figure 5. ^{Nat}Mo for a detector positioned at 26°. The ENDF/B-VII.1 library had the best agreement with the experimental data.

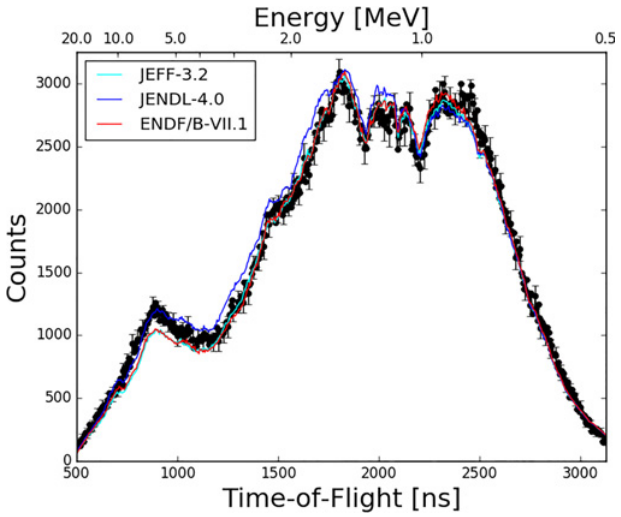

Figure 6. ^{Nat}Mo for a detector positioned at 108° . The ENDF/B-VII.1 library had better agreement than the JENDL-4.0 library, which overestimates the response between 2 MeV to 5 MeV.

^{Nat}Mo data and MCNP calculations are plotted in Fig. 5 and Fig. 6 for detectors positioned at 26° and 108°, respectively.

The FOM for the ENDF/B-VII.1 had the best agreement with 17 of 24 datasets, specifically detectors positioned at 26°, 73°, 108°, and 154°. The calculated FOMs were 2.08 and 2.00 for the 5 cm and 8 cm samples, respectively. The results for ENDF/B-VII.0 were nearly identical to ENDF/B-VII.1, and therefore not shown. The thicker sample was observed to have a lower FOM for this library and JEFF-3.2; however, it had a larger FOM for the JENDL-4.0 library, indicating that multiple scattering does not affect the observed differences in scattering.

JEFF-3.2 library was in agreement with 12 of the 24 datasets, and had the best agreement at 46° and 120°. For the JEFF-3.2 library the FOMs were 2.12 and 2.05 for the 5 cm and 8 cm samples, respectively. The JENDL-4.0 library had the worst agreement with the experimental data, with 5 of 24 datasets in agreement, having the best agreement at 90°. The calculated FOMs were 2.28 and 2.53 for the 5 cm and 8 cm samples, respectively.

6. Conclusions

Results from the ^{9}Be scattering experiments show that the JENDL-4.0 library had the best agreement with experimental datasets. For all libraries, the average FOM increased with the thicker beryllium samples.

The ENDF/B-VII.1 evaluation had the best agreement with the ^{Nat}Mo experimental data. However, an increase in ^{Nat}Mo sample thickness did not affect the FOM.

References

[1] D.P. Barry et al., "Quasi-differential Neutron Scattering in Zirconium from 0.5 to 20 MeV," Nucl. Sci. Eng. **174**(2), 188 (2013)
[2] F.J. Saglime, "High Energy Nuclear Differential Scattering Measurements for Beryllium and Molybdenum," Ph.D. dissertation, Mech. Aerospace and Nucl. Eng., Rensselaer Polytechnic Inst., Troy, NY (2009)
[3] A.M. Daskalakis et al., "Quasi-differential neutron scattering from ^{238}U from 0.5 to 20 MeV", Ann. Nucl. Energy **73**, 455 (2014)
[4] A.M. Daskalakis "Measurement of Elastic and Inelastic Neutron Scattering in the Energy Range from 0.5 to 20 MeV" Ph.D. dissertation, Mech. Aerospace and Nucl. Eng., Rensselaer Polytechnic Inst. Troy, NY (2015)
[5] A.E. Youmans et al., "Fast Neutron Scattering Measurements with Lead", 12th International Topical Meeting on Nuclear Applications of Accelerators (AccApp '15), Washington D.C., November 20, 2015
[6] M.B. Chadwick et al., "ENDF/B-VII.1 Nuclear Data for Science and Technology: Cross Sections, Covariances, Fission Product Yields and Decay Data," Nucl. Data Sheets **112**(12), 2887 (2011)
[7] OECD-NEA. (2015, July 9) JEFF-3.2. [Online]. Available: `https://www.oecd-nea.org/dbforms/data/eva/evatapes/jeff_32/`. Last accessed: June 29, 2016
[8] K. Shibata et al., "JENDL-4.0: A New Library for Nuclear Science and Engineering," J. Nucl. Sci. Technol. **48**(1), 1 (2011)
[9] G.F. Knoll, Radiation Detection and Measurement, 3rd ed., New York, NY: Wiley (2000)